Molecular Crystals and Liquid Crystals

Publication details, including instructions for authors and subscription information:
http://www.tandfonline.com/loi/gmcl20

Quasi-in-Plane Leaky Lasing Modes from Thin Waveguiding Layers of Nematic and Cholesteric Liquid Crystals

L. M. Blinov [a], S. P. Palto [a], V. V. Lazarev [a], G. Cipparrone [b], A. Mazzulla [b] & P. Pagliusi [b]

[a] Institute of Crystallography, Russ. Acad. Sci., Moscow, Russia

[b] Laboratorio Regionale LiCryL INFM-CNR, Physics Department, University of Calabria, Rende (CS), Italy

Version of record first published: 22 Sep 2010

To cite this article: L. M. Blinov, S. P. Palto, V. V. Lazarev, G. Cipparrone, A. Mazzulla & P. Pagliusi (2007): Quasi-in-Plane Leaky Lasing Modes from Thin Waveguiding Layers of Nematic and Cholesteric Liquid Crystals, Molecular Crystals and Liquid Crystals, 465:1, 37-50

To link to this article: http://dx.doi.org/10.1080/15421400701205404

Mol. Cryst. Liq. Cryst., Vol. 465, pp. 37–50, 2007

ISSN: 1542-1406 print/1563-5287 online
DOI: 10.1080/15421400701205404

Taylor & Francis
Taylor & Francis Group

Quasi-in-Plane Leaky Lasing Modes from Thin Waveguiding Layers of Nematic and Cholesteric Liquid Crystals

L. M. Blinov
S. P. Palto
V. V. Lazarev
Institute of Crystallography, Russ. Acad. Sci., Moscow, Russia

G. Cipparrone
A. Mazzulla
P. Pagliusi
Laboratorio Regionale LiCryL INFM-CNR, Physics Department, University of Calabria, Rende (CS), Italy

Lasing from dye doped liquid crystals was observed in the nematic, cholesteric and isotropic phases of liquid crystals in the plane waveguide geometry without mirrors and special modulation of the gain or refraction index by a holographic or other technique. The light was generated in a liquid crystal layer confined by two glasses with or without semitransparent electrodes, which formed an optical waveguide. A strong light amplification occurred along the narrow stripe produced by the pump beam with the necessary feedback provided by the walls of the waveguide. The lasing modes leaked into the glasses, were guided therein at very grazing angles and left the cell from its edges. The intensity and polarization of the lasing light depend on refraction indices of the liquid crystal and confining glasses. The conditions for lasing were discussed both analytically and numerically on the simplest example of the dye doped isotropic phase.

Keywords: dye lasers; liquid crystals; waveguides

The authors thank Prof. E. A. Luk'yanets and Dr. V.I. Alekseeva for supplying Chromene laser dye and Mr. A. Pane (LiCryL-CNR) for the help in experiment. The Russian group was supported by RFBR (grants no. 04-02-16466 and 05-02-16703) and Russian Federal Project (project 02.434.11.2025). The Italian group acknowledges the support from CNR-INFM and the CEMIF.CAL funds.

Address correspondence to L. M. Blinov, Institute of Crystallography, Russ. Acad. Sci., Leninsky pr.59, Moscow, Russia. E-mail: blinov@fis.unical.it

1. INTRODUCTION

The growing interest to lasing effect in dye doped liquid crystals [1–7] is stimulated by the prospects for building compact, all-organic mirrorless lasers with low threshold, tunability and high sensitivity to various external factors such as light, pressure, electric and magnetic fields, chemical species etc. Most of the papers devoted to the mirrorless laser generation from dye-doped liquid crystals deal with cholesteric [1–5] or smectic C^* [6] liquid crystals, which have helical structure. Therein, a periodic modulation of refractive index provides a distributed feedback necessary for the generation. There are also few works on nematic liquid crystals (NLC) [7] as well as on an isotropic liquid [8], in which the lasing was demonstrated using a periodic modulation of light amplification. In this case, an NLC is confined between two glasses forming a waveguide and illuminated with the interference (holographic) pattern produced by two powerful beams.

Recently [9] we have observed lasing in the same in-plane waveguide geometry but without special modulation of the gain or refraction index of NLC by a holographic or other technique. The corresponding lasing conditions were discussed both analytically and numerically in [10]. In our case, there are neither external mirrors nor cleaved surfaces playing the role of the mirrors in semiconductor lasers [11]. The light amplification occurred along the length of a narrow stripe produced by the pump beam and a feedback sufficient for generation was provided by the walls of the same waveguide. The lasing modes leaked into the glasses, were guided therein at very grazing angles and left the cell from its edges. The same leaky modes were also discussed with reference to luminescent solid organic films [12].

In this article we briefly resume the previous results and present new experimental data on the lasing in cholesteric liquid crystals (CLCs). In the case of a CLC, the lasing can be observed in the direction of both the helical axis (well known Bragg mode) and perpendicular to the helical axis, i.e., in the waveguiding direction, for which the distributed feedback is absent. The waveguiding modes are the same leaky modes observed in nematics and further on we shall call them Quasi In-Plane Leaky (or QIPL) modes.

2. EXPERIMENT

Materials

In the case of nematics, we used different materials and cells [9], however, here we discuss only typical examples. Our cells consist of

a pair of glasses of good quality (refractive index $n_g = 1.515$) with transparent conductive layers of indium-tin dioxide (ITO), which were covered with polyimide alignment layers. The layers were rubbed along the *y*-axis. The glasses were separated by Teflon stripes to form a gap of thickness $d = 6.3 \pm 0.3$ or $10 \pm 1\,\mu$m filled with a standard mixture E7 (BDH, clearing point 57°C, refraction indices $n_e \approx 1.73$, $n_o \approx 1.50$) doped with 0.5% of a dye Chromene (3-Diethylamino-7-imino-7H-chromene [3′,2′-3,4]pyrido[1,2a]-$(Et)_2$-benz-imidazole-6-carbonitryl) (NIOPIK, Moscow). The absorption band for Chromene in E7 was situated in the wavelength range of $\lambda = 450$–580 nm with two peaks at 515 and 560 nm. The dye reduced the clearing point of pure E7 mixture by 2°C.

In the case of cholesterics, we also used different cells and materials with different refraction indices. Our present experiment has been carried out on a chiral nematic mixture consisting of a 76% commercial nematic liquid crystal MLC6815 (Merck) and 24% chiral compound ZLI811 (Merck) doped with 0.5% dye 4-(Dicyanomethylene)-2-methyl-6-(4-dimethylamino-styryl)-4*H*-pyran (DCM, Aldrich). The maximum of DCM absorbance in this mixture was at $\lambda_m = 483$ nm and principal refraction indices at the lasing wavelength of $\lambda = 615$ nm were $n_\parallel \approx 1.52$ and $n_\perp \approx 1.47$ ($T = 25$°C). They have been found from the measurements of the s-and -p indices of the planar cholesteric texture $n_p = n_\perp$ and $n_s = [(n_\parallel^2 + n_\perp^2)/2]^{1/2}$ on an Abbe refractometer (Atago, model DTM-1) at $\lambda = 546$ nm and then corrected for the frequency dispersion. The pitch of the helical CLC structure $P \approx 397$ nm has been found from the refraction indices and the positions of the long- and short-wave edges of the Bragg band observed in the absorbance spectrum of the mixture, $\lambda_e = P\, n_\parallel \approx 604 \pm 2$ nm and $\lambda_o = P n_\perp \approx 583 \pm 2$ nm. A plane capillary cell was formed by two glasses ($n_g = 1.49$) covered with thin polyimide layers unidirectionally rubbed for homogeneous planar anchoring CLC at the surfaces. A 47 μm wide gap between the glasses was filled by the chiral mixture in the isotropic phase. During and after slow cooling, the glasses were gently shifted with respect to each other to provide a good quality shear-induced planar cholesteric texture.

Measurements

The cells were pumped (see Fig. 1) using the second harmonic of a Q-switched Nd:YAG laser (Continue Surelite-2). The *x*-polarized light beam was incident normally to the cell along the z-direction. The wavelength, pulse width and repetition rate were 532 nm, 5 ns and

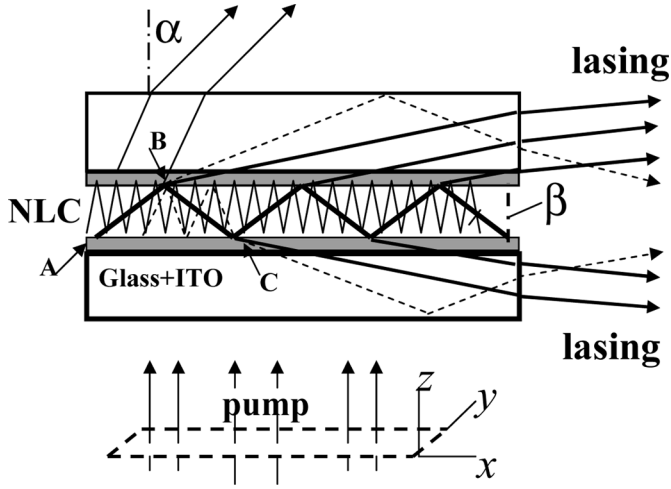

FIGURE 1 Waveguide NLC cell. Pump beam propagates along the z-direction and forms a 7×0.8 mm stripe in the *x,y*-plane of the cell. The light amplification appears in the LC layer along that stripe in the *x*-direction whereas waves are partially reflected by the boundaries between the liquid crystal and ITO covered glasses. Short period modes escape outward of the glasses without sufficient amplification for lasing. The amplified modes with larger period are guided by the glasses and exit from their butts.

5 Hz, respectively. The beam was focused by a cylindrical lens of 220 mm focal length into an almost rectangular narrow stripe of dimensions $x \times y = 7 \times 0.8$ mm. The cell was installed on a rotating stage and its plane (*x,y*) was adjusted to be vertical. The pump beam was directed normally to the cell plane (case of NLC, Fig. 1) or at $\theta = 45^\circ$ (case of CLC, Fig. 2) with respect to the cell normal z. The emission spectra were measured upon rotation of a photo-detector Ph through the angle ϕ around the vertical axis y, which passes through the centre of the focused pump beam. Actually, Ph is the input of a 0.6 mm diameter fibre connected to AvaSpec-2048 CCD spectrometer. The laser emission was observed above a well defined pump intensity threshold from the opposite butts of the cell following the longitudinal side of the irradiated spot. In case of CLC we could simultaneously measure both the Bragg mode (along the z-axis, $\phi = 0$) and QIPL modes close to the x-axis ($\phi \approx 90^\circ$). Between the cell and spectrometer, a polarizer and/or neutral filters were installed when needed.

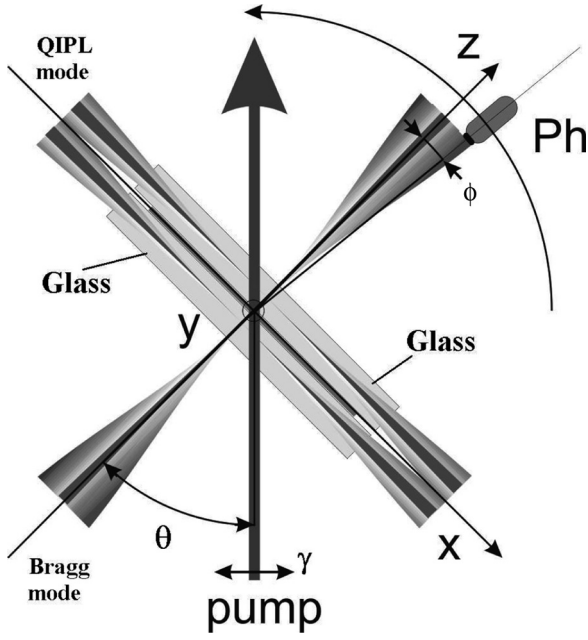

FIGURE 2 The top view on a cholesteric cell irradiated by the pump beam. Two pairs of QIPL lasing modes and two single Bragg lasing modes are shown.

3. EXPERIMENTAL RESULTS

The luminescence in the nematic phase (curve 1) and lasing emission spectra in the nematic (curve 2) and isotropic (curve 3) phases for the E7-Chromen mixture are shown in Figure 3. The lasing is observed at the long-wavelength slope of the luminescent curves where a typical fine multimode structure is seen. Its finess of about 1 nm is determined by the spectrometer resolution (0.5 nm). The lines within the group exchange by intensity from one pump pulse to another. The dependence of the emission intensity on the pump power has a threshold character typical of all lasing liquid crystals. In the nematic phase, the emission threshold within the same spectral location of the fluctuating modes can be controlled by a voltage applied to the ITO electrodes.

The angular dependence of the lasing emission intensity in the *x,z* plane is shown in the Inset to Figure 3 for the 10 μm thick cell filled with the same E7-Chromene mixture. In fact, the light exits from the cell being guided by two opposite glasses. The $\phi = 90^\circ$ line corresponds to the NLC plane *x,z*. The peaks 1 and 2 are asymmetric with

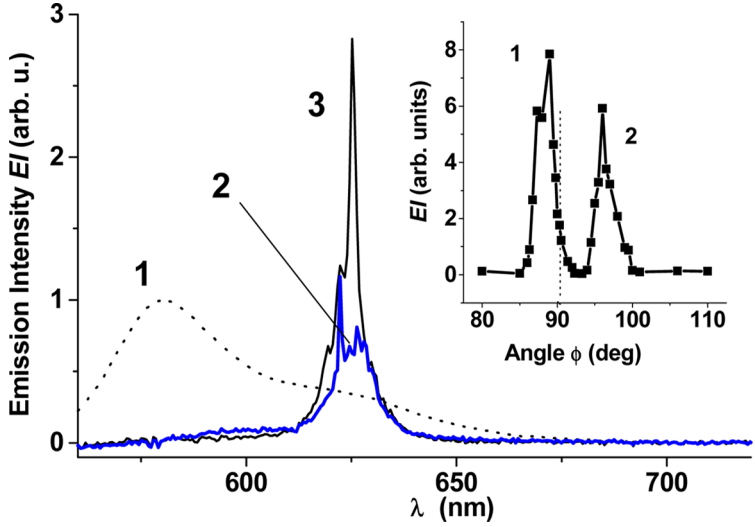

FIGURE 3 Spectrum of luminescence of Chromene in the E7 mixture measured in the cell of thickness $d = 6.3 \pm 0.5\,\mu m$ at low pump intensity (curve 1). The lasing emission intensity (*EI*) spectra of the same cell in the nematic phase (curve 2) and at a temperature above the transition to the isotropic phase (curve 3) The pump energy density is $P = 0.3\,mJ/cm^2$ pulse, no voltage applied. Inset. Angular dependence of the lasing emission intensity in the *x,z* plane (angle φ) for a cell of thickness $d = 10 \pm 1\,\mu m$ filled with the same E7-Chromene mixture ($P = 0.3\,mJ/cm^2$ pulse and applied voltage $U_{rms} = 7$ V, $P_{threshold} = 0.15\,mJ/cm^2$ pulse). The two peaks are situated at $\phi = 89$ and 96°. (See COLOR PLATE I)

respect to this line because the edges of the glasses are not precisely cut off. The light generation occurs in the NLC active layer, however, the glasses play very important role: they provide a selection of the proper lasing modes (see below) and the exit of the generated light from the cell.

Generally, our results obtained for the cholesteric liquid crystal are similar to that for the nematic but have some specific features. In Figure 4 we see the emission spectra measured upon excitation of the freshly made CLC cell by a pump beam of energy 8 μJ/pulse focused with a cylindrical length (energy density of 0.14 mJ/cm^{2}pulse). The circularly polarised Bragg mode is observed at an angle $\phi = 0$ along the cell normal, see Figure 2. The almost linearly s-polarised QIPL mode shown is emitted from the edge of a glass in the direction of the excited stripe at angle ϕ close to 90°. In fact, there are totally 4 leaky modes (from two glasses into two opposite directions

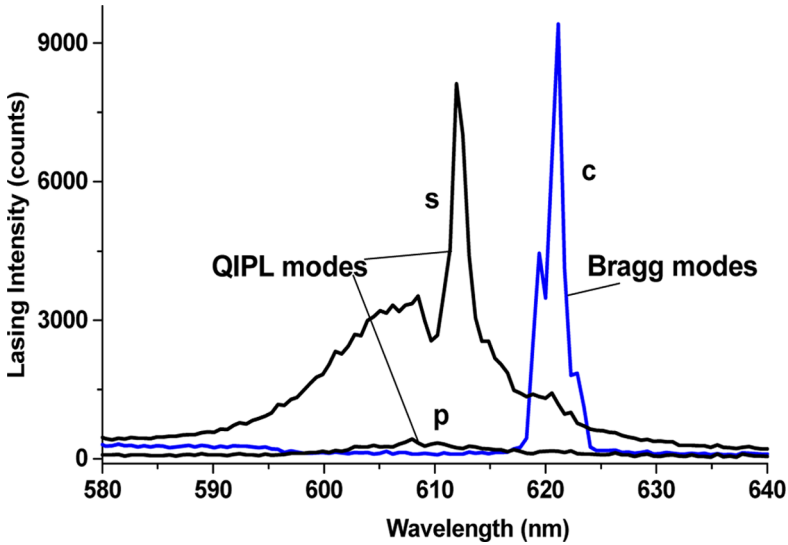

FIGURE 4 The emission spectra measured upon excitation of a CLC cell by a pump beam focused by a cylindrical length. The Bragg mode has circular polarization (c). The QIPL modes with s- and p-polarization are observed from the edge of a glass in the direction of the excited stripe. Pump pulse energy 8 μJ/pulse (energy density 0.14 mJ/cm^{2}pulse), T = 19°C. (See COLOR PLATE II)

as shown in Fig. 2) Note that both the Bragg and QIPL modes are observed simultaneously. Therefore, the QIPL modes provide a competing channel for light generation in cholesterics: when the size of the pump beam is extended in any transverse direction, due to strong amplification, a considerable amount of light energy leaks into that direction. Since the ordinate scales in Figure 4 have the same units for both curves, the overwhelming part of the energy leaks into the QIPL modes.

The angular dependencies of the QIPL mode emission intensity are shown in Figure 5. In this case, the measurements were made few weeks later on the same, somewhat aged cell and at a temperature of 28°C. Due to this, the position of the long wavelength edge of the Bragg band was shifted from 622 nm (Fig. 4) to 607 nm (Fig. 5, inset) and the threshold for lasing in the Bragg mode became considerably higher. The spectra of the emission of the aged cell in the Bragg and QIPL mode are shown in the Inset to Figure 5 at the pump energy density of 2.5 mJ/cm^{2}pulse. For the Bragg band, the pump density is still below the threshold and only luminescence is seen whereas the intensity of the QIPL mode is strong (note that the scale for this mode

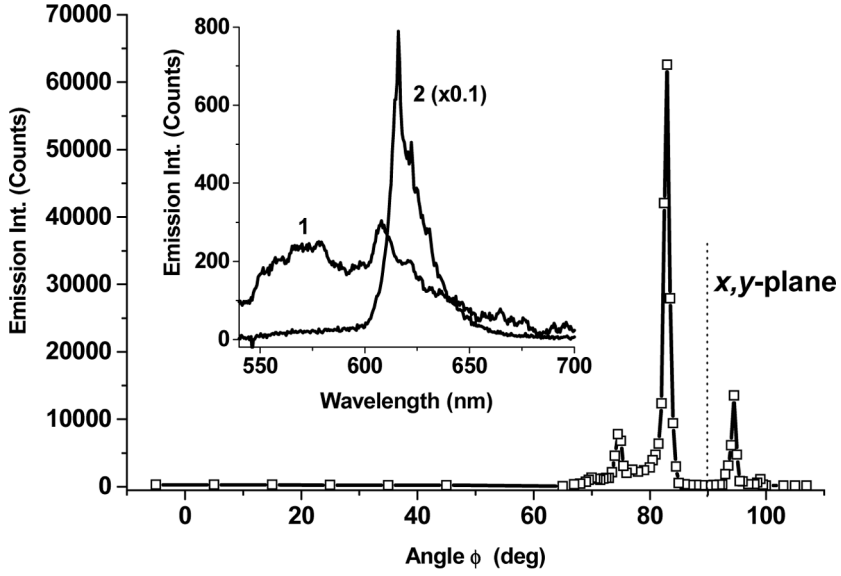

FIGURE 5 Inset. Spectra of dye luminescence in the normal Bragg mode (curve 1) and lasing in the QIPL mode (curve 2, scale reduced 10 times). Pump conditions: cylindrical lens, illuminated spot along x, pump energy density of 2.5 mJ/cm^{2}pulse. Main plot: Angular dependencies of the emission intensity at λ_{max} showing narrow angular QIPL modes (same pump conditions). T = 28°C.

is 10 times reduced). The spectral position of λ_{max} for the QIPL mode is almost the same for the fresh and aged cells (within 612–616 nm).

In the angular dependence shown in the main plot of Figure 5 we can distinguish four maxima located at 74.5, 83, 94.5 and 99°. The two strong maxima at 83 and 94.5° are strongly s-linearly polarised (TE), the two weaker ones are only partially p-polarised (TM). Each of the two TE-TM pairs exits from one glass at rather grazing angles with respect to the glass surfaces, e.g., $-15.6°$ (TM) and $-7°$ (TE). The TE modes have very small angular width, about 1° at the half-maximum. As in Figure 3, the angular maxima are not symmetric with respect to the middle x, z-plane of the cell at $\phi = 90°$ because the edges of the two glasses were not ideally cut although some asymmetry may also result from the non-uniform pump beam absorption along the z-axis.

4. DISCUSSION AND MODELLING

Since our experiment on the QIPL modes was carried out without special modulation of refractive index or amplification coefficient as

necessary for the distributed feedback [13], the question arises about the nature of the feedback for the laser generation. In principle, two menisci of the NLC layer may play the role of low-quality mirrors, however, we have excluded this possibility changing an angle between the illuminated stripe and the cell edges.

In order to understand the mechanism of low threshold lasing, consider the simplest example of waveguide modes in "cold" waveguide with parameters taken from the experiment for the isotropic phase of E7 doped with Chromen ($d = 6.3\,\mu\text{m}$, $n = 1.59$, Fig. 3). In the absence of absorption (positive or negative), due to the self-consistency condition for the guided eigen modes [11]

$$\cos\beta(m) = \frac{m\lambda_a}{2dn} \quad (m = 1, 2, 3, \ldots) \tag{1}$$

such a waveguide can support the infinite number of modes of different wavelength, e.g., it can guide white light. However, in experiment, the lasing is observed in air at $\lambda_{\text{a}} \approx 625\,\text{nm}$ (see curves 2 and 3 in Fig. 3), at which there are optimum conditions for light gain. For this λ_{a}, the "cold" waveguide supports 32 discrete modes for each polarization because $2dn/\lambda_{\text{a}} = 32.05$. The corresponding $\beta(m)$ angles for these modes are shown by open squares in Figure 6.

Now, remember that our isotropic layer is confined by two glasses. From angle $\beta(m)$ we can find the corresponding mode angles in the glasses β_{g} and air β_{a} using the Snell law,

$$n\,\sin\,\beta = n_g\,\sin\,\beta_g = \sin\,\beta_a \tag{2}$$

The angles β_{g} and β_{a} are shown in Figure 6 by filled squares and open circles, respectively. It is seen that modes with numbers $m = 10$–25 enter the glasses at angles $\beta_{\text{g}} = 41.07^\circ$ ($m = 25$)–85.85° ($m = 10$), are captured there due to the total internal reflection and leave glasses for air only from their edges.

These eigenmodes are of our interest and now we consider the conditions for their amplification found by the matrix method applied to the infinitely large thin waveguides [10]. In the particular case, the waveguide consists of an isotropic material (as before, $d = 6.3\,\mu\text{m}$, $n = 1.59$) with *negative absorption*, placed between infinitely thick non-absorbing glasses ($n_{\text{g}} = 1.515$). We calculate the angle dependent negative absorption coefficients $\alpha_{\text{s,p}}(\beta)$ satisfying the following condition: the complex light amplification coefficient A along the round trip from point A via point B to point C (Fig. 1) must identically be equal to 1, $A \equiv 1$ (subscripts s and p are referred to the s-and p-polarized eigen waves in the waveguide).

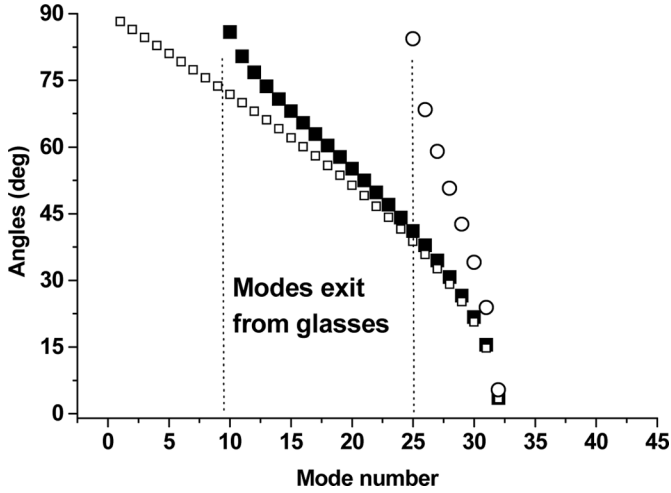

FIGURE 6 Angular waveguide modes with wavelength $\lambda_a = 625\,\text{nm}$ in the $6.3\,\mu\text{m}$ thick infinitely large non-absorbing isotropic layer of E7 with $n = 1.59$ confined between two glasses of refraction index $n = 1.515$. Open squares: angles β for all modes supported by the waveguide; filled circles: angles β_g for modes leaked from the E7 waveguide into two glasses; open circles: angles β_a for modes leaked from the glasses to air. Vertical dotted lines confine the modes entering the glass and captured there due to the total internal reflection.

$$\text{s-wave: } \left[\frac{\sin(\beta_g - \beta_s)}{\sin(\beta_g + \beta_s)}\right]^2 \cdot \exp\left[-\frac{\alpha_s d}{\cos\beta_s}\right] \cdot \exp\left(-i\frac{2n_s k_0 d\,\cos\beta_s}{n_g}\right) = 1$$

$$\text{p-wave: } \left[\frac{\tan(\beta_g - \beta_p)}{\sin(\beta_g + \beta_p)}\right]^2 \cdot \exp\left[-\frac{\alpha_p(\beta_p) d}{\cos\beta_p}\right] \cdot \exp\left(-i\frac{2n_p k_0 d\,\cos\beta_p}{n_g}\right) = 1 \tag{3}$$

These expressions have clear physical sense: the last multiplier (imaginary) corresponds to the phase self-consistency condition (1) $(n/n_g)(2\pi/\lambda_0)d\cos\beta = \pi m$,the central multiplier describes the light negative absorption along the round trip AB + BC in Figure 1 (factor 2 is included in α) and the first multiplier describes the Fresnel reflections at the waveguide-glass boundaries, which provide the feedback necessary for lasing (for details see [10]).

The result of the calculation is shown in Figure 7. For both light polarizations, with increasing angle, the absolute value of the negative absorption coefficient necessary for lasing tends to zero, that corresponds

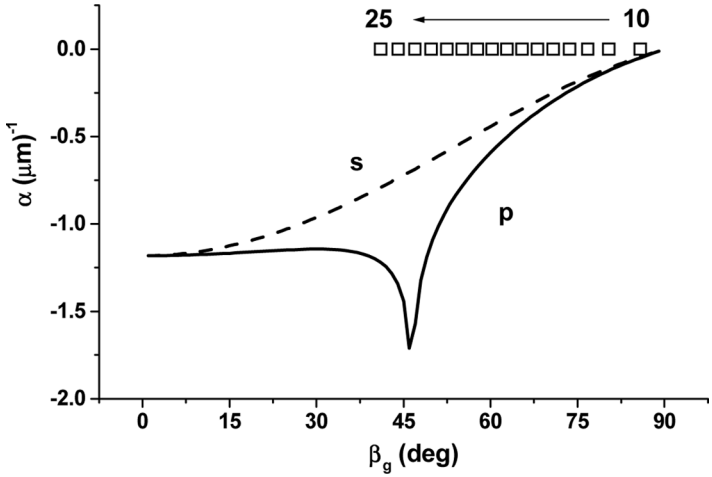

FIGURE 7 Calculated negative absorption coefficients necessary for the light generation on s- and p- leaky modes as functions of their eigen angles. The waveguide is formed by Iso-phase E7 ($n = 1.59$) between two glasses ($n = 1.515$). In the right-up corner are shown the numbers m of the modes in the glasses at proper angular positions.

to low threshold pump energy density. In other words, the most grazing mode ($m = 10$) has the lowest threshold. The reason for this is easily seen from Eq. (3). For example, for the s-mode, disregarding the phase term we can write

$$-\alpha_s = \frac{\cos\beta_s}{d} \ln\left[\frac{\sin(\beta_g + \beta_s)}{\sin(\beta_g - \beta_s)}\right]^2 \tag{4}$$

As follows from (4), factor $\cos\beta_s/d$ shows that thicker layers and wider angles β_s (grazing modes, $\beta_s \to \pi/2$) result in smaller α_s (lower pump threshold). In addition, the logarithm of Fresnel ratio, which shows the inverse of the feedback efficiency, is the largest for almost normal modes ($\beta_g \cong \beta_s$) and decrease about 7 times for $\beta_g \cong \pi/2$. Thus, according to Eq. (3) and Figure 7, the lowest threshold modes must be the most grazing modes, e.g. with number $m = 10$, 11 or 12. These QIPL modes propagate in glasses with eigen angles β_g ($m = 10$, 11, 12) $= 85.85$, 80.41 and 76.76°. The same modes in the waveguide propagate at β ($m = 10$, 11, 12) $= 72.29$, 69.97 and 68.05°, respectively.

Finally, using the procedure based on the precise numerical solution of the Maxwell equations [14], we have calculated explicitly the angular dependencies of the optical transmittance (T) for our

simplest waveguide. In the modelling, a probe beam in the form of a plane wave of different wavelength with unit intensity enters from glass the same isotropic waveguiding layer ($d = 6.3\,\mu m$, $n = 1.59$) with negative absorption coefficient $\alpha = -0.05\,\mu m^{-1}$ close to the threshold conditions. The light is amplified in the layer and then leaves it for the second glass. The transmittance (amplified intensity of the input beam) is virtually measured within the second glass at $\lambda_g = \lambda_a/n_g = 412.5\,nm$. For the normal light incidence ($\beta_g = 0$) the amplified transmittance (AT) has a sinusoidal form oscillating between 1.366 and 1.371 and showing one of the maxima at 626 nm. With increasing angle up to $\beta_g \approx 80^\circ$ AT increases gradually up to the values of about 6–7. The maxima become sharper and their positions depend on β_g. At larger angles, singularities of AT (lasing) appear at several wavelengths. In our experimental range they are observed at an angle of about $\beta_g = 85.5^\circ$ as shown in the inset to Figure 8 (the β_g was taken with a step of 0.5°). The strongest lasing line is observed at $\lambda_a = 626\,nm$. The neighbor two modes (at 567 and 696 nm) are outside of the experimental range. The angular dependence of AT is shown in

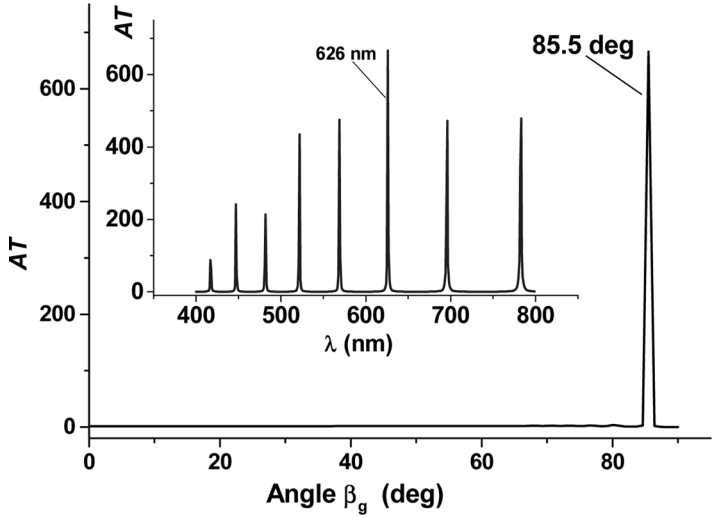

FIGURE 8 Calculated amplified transmittance (AT) as a function of the incidence angle β_g of the probe beam entering the waveguide ($d = 6.3\,\mu m$, $n = 1.59$, $\alpha = -0.05\,\mu m^{-1}$) from glass ($n_g = 1.515$). Calculated "resonance" angle in glass is $\beta_g = 85.5^\circ$, wavelength $\lambda_g = \lambda_a = 626/n_g\,nm$. Inset: Calculated spectrum of the amplified transmittance at an angle $\beta_g = 85.5^\circ$ (same parameters of the waveguide).

the main plot of Figure 8. We see that the strongest amplified mode ($\lambda_a = 626$nm, $AT = 670$) propagates at an angle of $\beta_g = 85.5 \pm 0.5^\circ$ in glass. Therefore, we conclude that it is the same QIPL mode with $m = 10$ shown in Figure 7 (propagating at $\beta_g = 85.85^\circ$). This mode propagates in both glasses at very grazing angle of $\beta'_g = \pm 3.15^\circ$ *with respect to the glass surfaces*. At the ideally cut edge it would exit the glass for air at an angle of $\beta'_a = \text{asin}(n_g \sin\ \beta'_g) = \pm 4.8^\circ$. Our angles $\beta'_a = -1$ and $+6^\circ$ (see Inset to Fig. 3) are not very far from this value despite the glasses were cut without any further treatment. We have also checked by modelling that the conductive ITO layers and aligning polyimide layers influence our basic results insignificantly.

Our modelling can also be applied to the case of a waveguide filled with the cholesteric liquid mixture (with $n_\parallel \approx 1.52$ and $n_\perp \approx 1.47$) discussed above (Figs. 4, 5). In particular, we have found that the calculated QIPL lasing modes in the waveguide formed by two glasses with $n_g = 1.49$ are strongly s-polarized. This is consisted with the fundamental condition for the allowed QIPL modes in a waveguide $n_s = [(n_\parallel^2 + n_\perp^2)/2]^{1/2} > n_g > n_p \approx n_\perp$, which is now fulfilled only for the s-modes.

5. CONCLUSION

In conclusion, we have observed lasing from dye doped nematic, cholesteric and isotropic phases of liquid crystals in the plane waveguide geometry without mirrors and special modulation of the gain or refraction index. The light was generated in a liquid crystal layer confined by two glasses with or without semitransparent electrodes, which formed an optical waveguide. The lasing modes leaked into the glasses, were guided therein at very grazing angles and left the cell from its edges (Quasi-In-Plane Leaky or QIPL modes). The intensity and polarization of the lasing light depend on refraction indices of the liquid crystal and confining glasses. The conditions for lasing were discussed both analytically and numerically on the simplest example of the dye doped isotropic phase. It was shown, that the lowest threshold for lasing is observed for the QIPL modes propagating in the waveguide at an angle just exceeding the total reflection angle of the waveguide. Therefore, in the glasses the same modes propagate very close to the interface between the waveguide and glass.

REFERENCES

[1] Il'chishin, I., Tikhonov, E., Tishchenko, V., & Shpak, M. (1980). *JETP Lett.*, *32*, 24.
[2] Kopp, V. I., Zhang, Z.-Q., & Genack, A. (2003). *Progr. Quant. Electron.*, *27*, 369.
[3] Cao, W., Munos, A., Palffy-Muhoray, P., & Taheri, B. (2002). *Nature Mater.*, *1*, 111.

[4] Chanishvili, A., Chilaya, G., Petriashvili, G., Barberi, R., Bartolino, R., Cipparrone, G., Mazzulla, A., Gimenes, R., Oriol, L., & Pinol, M. (2005). *Appl. Phys. Lett.*, *86*, 051107.
[5] Strangi, G., Barna, V., Caputo, R., de Luca, A., Versace, C., Scaramuzza, N., Umeton, C., Bartolino, R., & Price, G. (2005). *Phys. Rev. Lett.*, *94*, 063903.
[6] Ozaki, M., Kasano, M., Kitasho, T., Ganske, D., Haase, W., & Yoshino, K. (2003). *Adv. Mater. Weinheim Ger.*, *15*, 974.
[7] Matsui, T., Ozaki, M., & Yoshino, K. (2003). *Appl. Phys. Lett.*, *83*, 422.
[8] Lo, D., Ye, C., & Wang, J. (2003). *Appl. Phys.*, *B76*, 649.
[9] Blinov, L. M., Cipparrone, G., Lazarev, V., Mazzulla, A., & Pagliusi, P. (2006). *Appl. Phys. Lett.*, *89*, 031114.
[10] Palto, S. P. (2006). *JETP*, *103*, no. 8, 472.
[11] Saleh, B. E. A. & Teich, M. C. (1991). *Fundamentals of Photonics*, J. Wiley & Sons: New York.
[12] Penzkofer, A., Holzer, W., Tillmann, H., & Hörhold, H.-H. (2004). *Opt. Commun.*, *229*, 279.
[13] Kogelnik, H. & Shank, C. V. (1972). *J. Appl. Phys.*, *43*, 2327.
[14] Palto, S. P. (2001). *JETP*, *92*, 552.